

# Synthesis and structural characterisation of redox-responsive *N*-ferrocenoyl amino acid esters; the X-ray crystal structure of *N*-ferrocenoyl alanine methyl ester; electrochemical anion recognition and <sup>1</sup>H NMR complexation studies

Michael J. Sheehy <sup>a</sup>, John F. Gallagher <sup>a,\*</sup>, Mashita Yamashita <sup>b</sup>, Yoshiteru Ida <sup>c</sup>, Jennifer White-Colangelo <sup>d</sup>, Jeremi Johnson <sup>d</sup>, Ron Orlando <sup>d</sup>, Peter T.M. Kenny <sup>a,\*</sup>

<sup>a</sup> School of Chemical Sciences, Dublin City University, Dublin 9, Ireland

<sup>b</sup> Kyushu Laboratories, Yoshitomi Pharmaceutical Industries Ltd., Yoshitomi-cho, Chikujo-gun, Fukuoka 871-8550, Japan

<sup>c</sup> School of Pharmaceutical Science, Showa University, Hatanodai, Shinagawa-ku, Tokyo 142-8555, Japan

<sup>d</sup> Complex Carbohydrate Research Center, University of Georgia, 220 Riverbend Road, Athens, GA 30602-4712, USA

## Abstract

The *N*-ferrocenoyl amino acid ester derivatives FcCOR {Fc = (η<sup>5</sup>-C<sub>5</sub>H<sub>5</sub>)Fe(η<sup>5</sup>-C<sub>5</sub>H<sub>4</sub>)} where R = Gly(OMe) **1**, Gly(OEt) **2**, Gly(OBn) **3**, L-Ala(OMe) **4**, L-Ala(OEt) **5**, L-Leu(OMe) **6**, L-Leu(OEt) **7**, L-Leu(OBn) **8**, L-Phe(OMe) **9** and L-Phe(OEt) **10**, were prepared by coupling ferrocene carboxylic acid with the appropriate amino acid ester starting materials using the 1,3-dicyclohexylcarbodiimide (DCC), 1-hydroxybenzotriazole (HOBt) protocol and these have been characterised by spectroscopic techniques. The electrochemical anion sensing behaviour of compounds **1–10** with several anions using a platinum microdisk working electrode is described, together with <sup>1</sup>H NMR anion complexation studies. The X-ray single crystal structure of *N*-ferrocenoyl-L-alanine methyl ester **4** has been determined and contains two molecules which differ slightly in conformation in the asymmetric unit of space group P2<sub>1</sub> (No. 4); principal dimensions are amide N(H)C=O 1.224(6) and 1.231(6) Å, ester C=O 1.220(10) and 1.190(7) Å, with N–H···O=C(amide) as the primary intermolecular hydrogen bond, N···O 2.992(6) and 2.971(6) Å and with graph set C(4).

© 2004 Elsevier B.V. All rights reserved.

**Keywords:** Ferrocene; Electrochemistry; Platinum microdisk electrode; <sup>1</sup>H NMR coordination studies; X-ray crystal structure

## 1. Introduction

The design and synthesis of novel molecular receptors to complex and electrochemically recognise anionic guest systems is of current scientific interest [1]. The coordination of guest species is a major research area in molecular recognition chemistry with the ultimate aim of understanding fundamental biological processes [2,3]. Transition metal complexes, such as ferrocene derivatives, have found a variety of applications in molecular

sensors, charge transfer chemistry and peptide mimetic models [3–9]. The majority of organometallic derivatives employed in anion receptor research contain a ferrocenyl (Fc) or a ferrocenoyl (FcCO) moiety with a pendant macrocyclic group as integral components for recognition and binding studies. Research studies have also focussed on 1,1'-metallocenyl derivatives where extensive hydrogen bonding can occur between the 1,1'-substituents. Reports on the incorporation of a ferrocene group onto proteins have shown the mediation of electron transfer between electrodes and the protein redox sites [2,10]. Recently, the synthesis and characterisation of several unusual *N*-ferrocenoyl and *N*-ferrocenyl amino acid and peptide derivatives has been reported [11–27].

\* Corresponding authors. Tel.: +353-1-7005-689 (P.T.M. Kenny), +353-1-7005-114 (J.F. Gallagher); fax: +353-1-7005-503 (P.T.M. Kenny).

E-mail addresses: [John.Gallagher@dcu.ie](mailto:John.Gallagher@dcu.ie) (J.F. Gallagher), [peter.kenny@dcu.ie](mailto:peter.kenny@dcu.ie) (P.T.M. Kenny).

We now report the synthesis and spectroscopic characterisation of a series of *N*-ferrocenoyl amino acid esters,  $\text{FcCOR}$  {Fc =  $(\eta^5\text{-C}_5\text{H}_5)\text{Fe}(\eta^5\text{-C}_5\text{H}_4)$ } where R = Gly(OMe) **1**, Gly(OEt) **2**, Gly(OBn) **3**, L-Ala(OMe) **4**, L-Ala(OEt) **5**, L-Leu(OMe) **6**, L-Leu(OEt) **7**, L-Leu(OBn) **8**, L-Phe(OMe) **9** and L-Phe(OEt) **10**. The electrochemical properties of these unnatural amino acid esters as anion receptors has been investigated using a platinum microdisk working microelectrode which represents a relatively new departure from the widespread use of conventional platinum macroelectrodes in metal-organic analytical studies (electrochemical details in experimental). The  $^1\text{H}$  NMR anion coordination properties of compounds **1–10** are also reported, and the X-ray crystal structure of *N*-ferrocenoyl alanine methyl ester **4** has been determined for comparison with related structures [7,12] and the reported *N*-ferrocenoyl glycine ester derivatives [14,28]. The benefit of such crystal structure analysis is that it can provide an understanding of the possible interactions present in the structure of a potential anion receptor as well as yield valuable information for hydrogen binding modes and binding sites in solution studies.

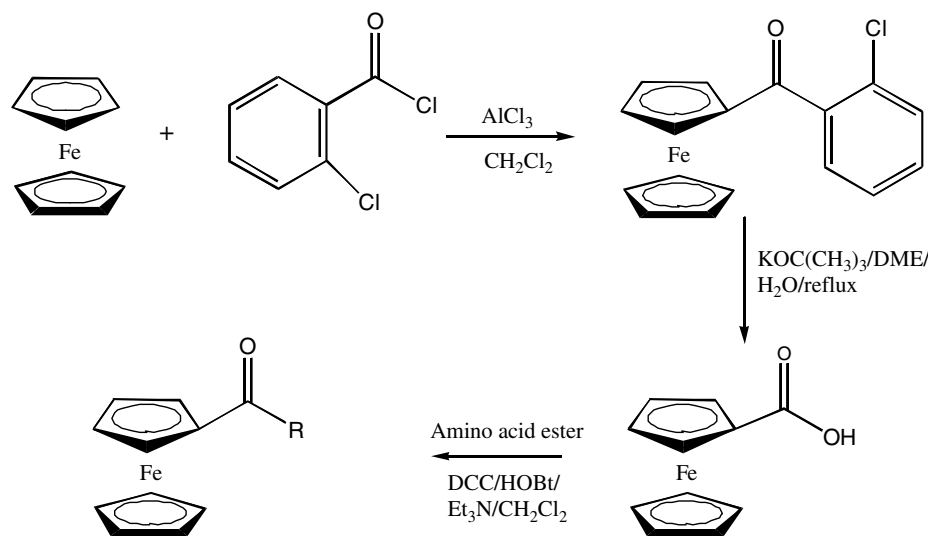
## 2. Results and discussion

### 2.1. Synthesis

The synthesis of the ferrocenoyl amino acid ester derivatives **1–10** was successfully carried out by reaction of ferrocene carboxylic acid [29] and the appropriate amino acid ester [30] under basic conditions in the presence of dicyclohexylcarbodiimide (DCC) and 1-hydroxybenzotriazole (HOBt). The procedure is related to

that used by Degani and Heller to incorporate ferrocene carboxylic acid onto proteins [2]. Condensation of ferrocene carboxylic acid with esters of the amino acids, glycine, L-alanine, L-leucine and L-phenylalanine cleanly led to the formation of orange to yellow coloured ferrocenoyl amino acid ester derivatives in good yield (Scheme 1). The compounds are reasonably stable however they slowly decompose over a period of time. Crystals suitable for X-ray crystallographic analysis were obtained for compounds **1** [14], **3** [28] and **4**. The products were characterised by spectroscopic techniques prior to the electrochemical studies to confirm their structures.

The  $^1\text{H}$  and  $^{13}\text{C}$  NMR spectra for compounds **1–10** showed peaks in the ferrocene region characteristic of a mono-substituted ferrocene subunit [7]. For example, in the case of the glycine derivatives **1**, **2** and **3** the unsubstituted  $\eta^5\text{-C}_5\text{H}_5$  ring appears as a singlet in the  $^1\text{H}$  NMR spectra at  $\delta$  4.23,  $\delta$  4.24 and  $\delta$  4.22, respectively. The NH proton is present as a triplet at  $\delta$  8.25,  $\delta$  8.22 and  $\delta$  6.21 and the  $\text{-NHCH}_2\text{CO-}$  protons appear as doublets at  $\delta$  3.90 ( $J = 6$  Hz) for **1**,  $\delta$  4.15 ( $J = 5$  Hz) for **2** and  $\delta$  4.18 ( $J = 5$  Hz) for **3**. Selected  $^1\text{H}$  NMR spectroscopic data for several of the ferrocenoyl amino acid esters are presented in Table 1. The protons in the *ortho* position on the substituted  $\eta^5\text{-C}_5\text{H}_4$  ring appear in the region  $\delta$  4.59–4.78 whereas the protons in the *meta* position occur in the chemical shift range  $\delta$  4.32–4.41. The unsubstituted  $\eta^5\text{-C}_5\text{H}_5$  ring system is observed as a singlet for all of the compounds **1–10** in the chemical shift range  $\delta$  4.12–4.29. The  $^{13}\text{C}$  NMR spectra display signals in the region  $\delta$  67.2–75.6 indicative of a mono-substituted ferrocene subunit with the *ipso* carbon of the substituted Cp ring appearing in a narrow range of  $\delta$  75.0–75.6.



Scheme 1. Synthesis of *N*-ferrocenoyl amino acid esters **1–10**; R = Gly(OMe) **1**, Gly(OEt) **2**, Gly(OBn) **3**, L-Ala(OMe) **4**, L-Ala(OEt) **5**, L-Leu(OMe) **6**, L-Leu(OEt) **7**, L-Leu(OBn) **8**, L-Phe(OMe) **9** and L-Phe(OEt) **10**.

Table 1  
Selected  $^1\text{H}$  NMR spectroscopic data for a number of *N*-ferrocenoyl amino acid derivatives ( $\text{CDCl}_3$ ,  $\delta$  in ppm, room temperature)

| Compound | NH   | CH <sup>a</sup> | Cp <sup>ortho</sup> | Cp <sup>meta</sup> | Cp   |
|----------|------|-----------------|---------------------|--------------------|------|
| 3        | 6.21 | 4.18            | 4.69                | 4.34               | 4.22 |
| 4        | 6.25 | 4.69–75         | 4.64,<br>4.72       | 4.32               | 4.2  |
| 6        | 6.03 | 4.74–8          | 4.64,<br>4.71       | 4.33               | 4.21 |
| 8        | 6.04 | 4.82–7          | 4.65,<br>4.72       | 4.35               | 4.21 |
| 9        | 6.05 | 5.01–6          | 4.59,<br>4.63       | 4.32               | 4.12 |
| 10       | 6.08 | 4.99–<br>5.04   | 4.59,<br>4.63       | 4.33               | 4.13 |

<sup>a</sup> Hydrogen at  $\alpha$ -carbon.

## 2.2. $^1\text{H}$ NMR anion titration experiments

$^1\text{H}$  NMR spectroscopic studies were performed to investigate the interaction between the neutral *N*-ferrocenoyl amino acid derivatives and various anions. A solution of the compound was prepared at concentrations typically of the order of  $0.01 \text{ mol dm}^{-3}$  in  $\text{CDCl}_3$ . After each addition of anion, the  $^1\text{H}$  NMR spectrum was recorded and the changes in the chemical shift of the amide protons were noted. The result of the experiments was a plot of displacement in chemical shift of the amide proton as a function of the quantity of anion added. The *N*-ferrocenoyl glycine esters **1–3** exhibited some significant solution interactions with the anions. Noteworthy downfield shifts of the respective amide ( $-\text{CONH}-$ ) protons, ranging from ca.  $\delta$  0.5–2.5 ppm, were exhibited by the *N*-ferrocenoyl glycine esters **1–3** on addition of various anions as their tetrabutylammonium salts,  $[\text{Bu}_4\text{N}^+\text{X}^-]$  ( $\text{X}^- = \text{HSO}_4^-, \text{Br}^-, \text{Cl}^-$  and  $\text{H}_2\text{PO}_4^-$ ) to  $\text{CDCl}_3$  solutions. This observation agrees with previous reports and strongly suggests the contribution of the amide proton as a hydrogen donor in anion binding in solution [31]. The *N*-ferrocenoyl glycine methyl ester **1** is shown to sense halides and dihydrogen phosphate ( $\text{H}_2\text{PO}_4^-$ ) guest anions, the trend being  $\text{Cl}^- \gg \text{H}_2\text{PO}_4^- > \text{Br}^-$  (Fig. 1) and a similar overall trend was also observed for the ethyl **2** and benzyl esters **3**. These results suggest that a significant amide  $-\text{CO}-\text{NH}\cdots(\text{anion})^-$  hydrogen bonding interaction is contributing to the anion coordination process [1]. In contrast to this the *N*-ferrocenoyl-L-alanine esters **4** and **5** were found to elicit marginal downfield perturbations of the respective amide proton ranging from ca.  $\delta$  0.25–0.6 ppm. Negligible shifts were observed under identical experimental conditions with the other *N*-ferrocenoyl amino ester derivatives **6–10**. This strongly suggests that the amide hydrogen bonding interaction with the anion is relatively sterically hindered within the ferrocenoyl amide *niche* and is optimally available for hydrogen bonding interactions when the *N*-ferrocenoyl amino acid ester

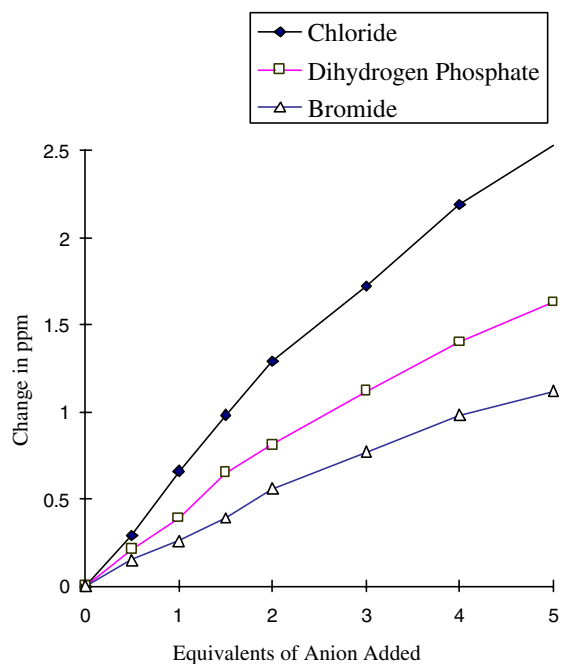


Fig. 1.  $^1\text{H}$  NMR titration curve of *N*-ferrocenoyl glycine methyl ester **1** with various anions added as their  $[\text{tBu}_4\text{N}]^+$  salts in  $\text{CDCl}_3$  at room temperature.

derivatives contain the simplest and least sterically hindered amino acid, glycine [6].

## 2.3. Electrochemical studies

The electrochemical behaviour of the ferrocene–ferrocenium oxidation wave is relatively insensitive to the amino acid R group, the  $E_{1/2}$  being in the range 590–610 mV. The behaviour of the *N*-ferrocenoyl amino acid esters **1–10** as potential anion receptors was investigated using microelectrochemical methods and a preliminary account of this work has been published [14]. Established methods of measuring electrochemical responses in inorganic-based anion sensors have typically used macroelectrodes for conventional measurements. Microelectrodes with dimensions in the micrometer range ( $\mu\text{m}$ ) possess some significant advantages over their macroscopic counterparts (mm) in electrochemical measurements, e.g. small currents, steady-state responses and short response times (for studying ultra-fast processes). As the current measured at an electrode is a function of the area, the current observed at microelectrodes lie in the *pico-* and *nanoampere* range, which are several orders of magnitude smaller than those measured using macroelectrodes. Some other advantages that microelectrodes have over macroelectrodes are rapid mass transport, small double layer capacitance and small ohmic drop, while an increased signal to noise ratio, a steady-state time independent response and higher sensitivity have also been noted. With a view to recognising minute quantities of anions and the ultimate

aim of in vivo measurements, these microelectrodes offer a relatively non-invasive means of monitoring, by being small, hence less tissue damage, but also because of the small concentrations of material electrolysed. For our measurements, these microelectrodes have been employed as analytical probes to measure the electrochemical response of several anions interacting with compounds **1–10**. The electrochemical measurements were recorded after progressively adding stoichiometric equivalents of anion guests (10 equiv.) as their tetrabutylammonium salts to solutions of the derivatives **1–10**. The electrochemical anion recognition properties for all of the *N*-ferrocenoyl amino acid esters are outlined in Table 2. The magnitude of the electrochemical shift on the  $E_{1/2}$  potential of *N*-ferrocenoyl glycine methyl ester **1** upon addition of the various anions is shown in Fig. 2. As depicted in this figure, the  $\text{HSO}_4^-$ ,  $\text{Cl}^-$  and  $\text{H}_2\text{PO}_4^-$  anions all produced negative shifts on the  $E_{1/2}$  potential on addition to the various *N*-ferrocenoyl amino acid solutions. The  $\text{BF}_4^-$  anion produced the only observed

positive perturbation. This is possibly due to the fact that the Fe atom is sensing the positively charged boron atom, hence the anodic shift. The dihydrogen phosphate anion ( $\text{H}_2\text{PO}_4^-$ ) produced the largest magnitude of negative perturbation of the ferrocene–ferrocenium redox couple of up to 120 mV with the host *N*-ferrocenoyl glycine methyl ester derivative **1**. The electrochemical findings complement the results obtained from the  $^1\text{H}$  NMR titration experiments where *N*-ferrocenoyl glycine methyl ester **1** exhibited the largest magnitude of amide proton shift. Thus compound **1** may have potential for the development of a novel electrochemical sensory device for the detection of the  $\text{H}_2\text{PO}_4^-$  anion. The results, however, also highlight the interaction of the ferrocenoyl unit with the anions as the order of perturbation changes depending on which analytical technique is utilised. This should not be surprising given that the two different analytical techniques are being used to probe different moieties within the electroactive sensor namely the amide N–H for the  $^1\text{H}$  NMR titration experiments and the ferrocene moiety for the electrochemical perturbation measurements. It was not possible to measure the effect of the bromide anion as bromide oxidation occurred at the  $E_{1/2}$  potential of the *N*-ferrocenoyl amino acid derivatives and there was little or no electrochemical shift of the ferrocene oxidation potential observed on addition of the perchlorate anion ( $\text{ClO}_4^-$ ).

From analysis of the results obtained in this investigation it is evident that replacing the amino acid has little effect on the  $E_{1/2}$  potential. Likewise changing from methyl to the ethyl and benzyl esters has little bearing on the  $E_{1/2}$  potential. This should not be surprising given that both the amino acid and ester functional groups are not in close proximity to the electroactive ferrocenoyl core. An important feature in the design of novel receptors is the incorporation of a redox center in close proximity to the anion coordination site. This gives the receptor the capability of electrochemically sensing anionic guest species as coordination will perturb the electrochemical response of the receptor. The perturbation of the electrochemical properties (ferrocene oxidation wave) of *N*-ferrocenoyl amino acid esters in the presence of various anions suggests their application in the construction of simple molecular sensors. The data presented for several anions in Table 2 show that compounds **1–10** recognise a variety of anions.

Beer et al. [32] have reported comparable  $\text{H}_2\text{PO}_4^-$  shifts to our results in a series of neutral and cationic macrocyclic heterobimetallic complexes. Further electrochemical studies are in progress to investigate the properties of some related *N*-ferrocenoyl dipeptide ester derivatives as anion sensors.

Microelectrodes are widely used as in vivo analytical probes [33]. The imprinting of such a receptor onto a polymeric support and subsequent bonding to the end of a microelectrode would produce an electrochemical

Table 2  
Electrochemical data<sup>a</sup> for **1–10** with electrochemical anion recognition properties<sup>b</sup>

| Compound  | $E_{1/2}$<br>(mV) | $\Delta E$<br>( $\text{HSO}_4^-$ ) | $\Delta E$<br>( $\text{Cl}^-$ ) | $\Delta E$<br>( $\text{H}_2\text{PO}_4^-$ ) | $\Delta E$<br>( $\text{BF}_4^-$ ) (mV) |
|-----------|-------------------|------------------------------------|---------------------------------|---|--|
| <b>1</b>  | 603               | –25                                | –20                             | –120  | 15                                     |
| <b>2</b>  | 601               | –30                                | –20                             | –95   | 20                                     |
| <b>3</b>  | 604               | –15                                | –15                             | –110  | 20                                     |
| <b>4</b>  | 599               | –25                                | –25                             | –90   | 30                                     |
| <b>5</b>  | 598               | –25                                | –25                             | –85   | 25                                     |
| <b>6</b>  | 603               | –20                                | –25                             | –90   | 25                                     |
| <b>7</b>  | 608               | –15                                | –25                             | –90   | 25                                     |
| <b>8</b>  | 607               | –30                                | –35                             | –85   | 25                                     |
| <b>9</b>  | 607               | –20                                | –30                             | –95   | 20                                     |
| <b>10</b> | 606               | –20                                | –35                             | –90   | 25                                     |

<sup>a</sup> See electrochemistry section in Section 4 for conditions.

<sup>b</sup> Shifts in the ferrocene–ferrocenium redox couple produced by the presence of anion (10 equiv.) added as their [ $n\text{Bu}_4\text{N}$ ]<sup>+</sup> salts.

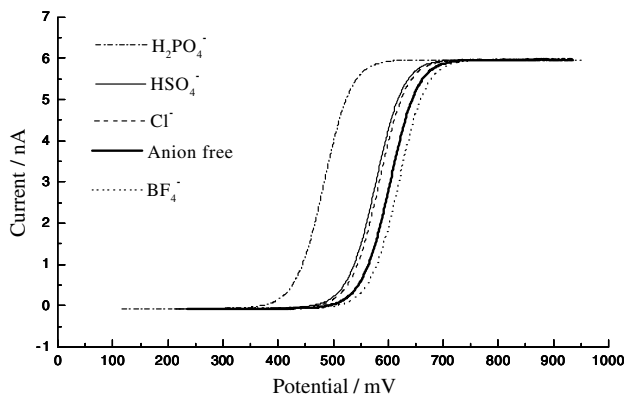


Fig. 2. Linear sweep voltammograms of **1** at a microdisk electrode in the presence of various anions added as their [ $n\text{Bu}_4\text{N}$ ]<sup>+</sup> salts. Supporting electrolyte: 0.1 mol dm<sup>-3</sup> [ $n\text{Bu}_4$ ]PF<sub>6</sub>, scan rate: 50 mV s<sup>-1</sup> (error +/- 5 mV).

anion sensor [34,35]. Such a device would have huge applications in determining the pH balance of the kidneys of which the  $\text{H}_2\text{PO}_4^-$  anion is produced. In the future it is hoped that subtle binding site modifications of such receptors can lead to dramatic fundamental changes in anion recognition properties and selectivity series.

#### 2.4. X-ray crystallographic studies of **4**

The crystal structure of **4** has been determined with selected bond lengths and angles listed in Table 3 (pertinent crystallographic details are contained in Section 4.4), the two independent molecules of **4** in the asymmetric unit are depicted in Fig. 3 and a packing diagram is present in Fig. 4. The structure can be directly compared with the glycine methyl and benzyl esters that have been communicated previously by the authors [14,28] and related structures that are available in the literature [7,12].

Compound **4** crystallises in the monoclinic system. The space group  $\text{P}2_1$  (No. 4) was deduced from the systematic absences and confirmed by the crystal structure analysis. The structure was solved using the Patterson function and refined by full-matrix least squares techniques. The hydrogen atoms were treated as riding atoms with C–H distances in the range 0.93–0.98 Å; the hydrogen atom bonded to nitrogen was refined to N–H = 0.75(2) Å. It was evident during the penultimate stage of refinement (when  $R[F_2 > 2\sigma(F^2)]$  was 0.075) that there were two types of disorder associated with the two independent molecules of **4**. The ester carbonyl oxygen atom of molecule A is disordered over two sites O2A/O2C with site occupancy factors of 0.76(2)/0.24(2),

respectively; the  $\eta^5\text{-C}_5\text{H}_5$  ring of molecule B is disordered over two positions with occupancies of 0.66(5)/0.34(5), respectively. These were treated with appropriate restraints and coordinates for the final refinement cycles, were refined with anisotropic displacement parameters in the final least squares calculations. The final *R*-factor is 0.030 for 1832 observed reflections [ $I > 2\sigma(I)$ ] out of a total of 2448 measured reflections.

In compound **4** the principal dimensions are amide N(H)C=O 1.224(6) and 1.231(6) Å, ester C=O 1.220(10) and 1.190(7) Å for the two independent molecules A and B (Table 3). The primary angle differences are between the substituted cyclopentadienyl ring and the amide C=ON–C plane, 14.8(4)° in molecule A and 2.7(5)° in B, as evidenced in Fig. 3. The primary intermolecular linkage is the N–H···O=C(amide) hydrogen bond which has N···O distances of 2.992(6) [N1A···O1B] and 2.971(6) Å [N1B···O1A<sup>#</sup>, # = 1 + *x*, *y*, *z*] and with graph set C(4). This involves the molecules linked in a one-dimensional chain as (A···B···A···B···) along the *a*-axis as depicted in Fig. 4. These N–H···O=C interactions are assisted by ( $\eta^5\text{-C}_5\text{H}_4$ )C–H···O=C interactions and involving an *ortho*-C–H unit to the same neighbouring carbonyl oxygen atom with graph set R<sub>1</sub><sup>2</sup>(7). The C6A···O1B and C6B···O1A distances are 3.341(7) and 3.425 Å. The reasons for two molecules being present in the asymmetric unit presumably arise due to molecular conformations being unable to sustain a growing linear chain through hydrogen bonding without having to adjust to accommodate it: this results in the observed (A···B···A···B···) chain in the crystal structure of **4**.

The molecular structure of **4** can be directly compared with the related glycine ester analogues [14,28],

Table 3  
Selected molecular dimensions (Å, °) for **4**

|                                    |           |            |          |       |
|------------------------------------|-----------|------------|----------|-------|
| O1A–C11A                           | 1.224(6)  | O1B–C11B   | 1.231(6) |       |
| O2A–C14A                           | 1.220(10) | O2B–C14B   | 1.190(7) |       |
| O2C–C14A                           | 1.43(4)   |            |          |       |
| O3A–C14A                           | 1.279(9)  | O3B–C14B   | 1.302(8) |       |
| O3A–C15A                           | 1.451(10) | O3B–C15B   | 1.448(8) |       |
| N1A–C11A                           | 1.334(7)  | N1B–C11B   | 1.326(7) |       |
| N1A–C12A                           | 1.437(7)  | N1B–C12B   | 1.447(7) |       |
| Cg(1)–Fe1A                         | 1.6468    | Cg(3)–Fe1B | 1.6295   |       |
| Cg(2)–Fe1A                         | 1.6366    | Cg(4)–Fe1B | 1.6442   |       |
| Cg(1)–Fe1A–Cg(2)                   | 177.77    |            |          |       |
| Cg(3)–Fe1B–Cg(4)                   | 174.78    |            |          |       |
| <i>Intermolecular interactions</i> |           |            |          |       |
| D–H···A                            | D–H       | H···A      | D···A    | angle |
| N1A–H1A···O1B                      | 0.86      | 2.149      | 2.992(6) | 167   |
| N1B–H1B···O1A                      | 0.86      | 2.140      | 2.970(6) | 162   |
| C6A–H6A···O1B                      | 0.93      | 2.553      | 3.341(7) | 143   |
| C6B–H6B···O1A                      | 0.93      | 2.571      | 3.425(7) | 153   |
| C8A–H8A···O2B                      | 0.93      | 2.556      | 3.401(8) | 151   |
| C8B–H8B···O1A                      | 0.93      | 2.484      | 3.406(7) | 171   |

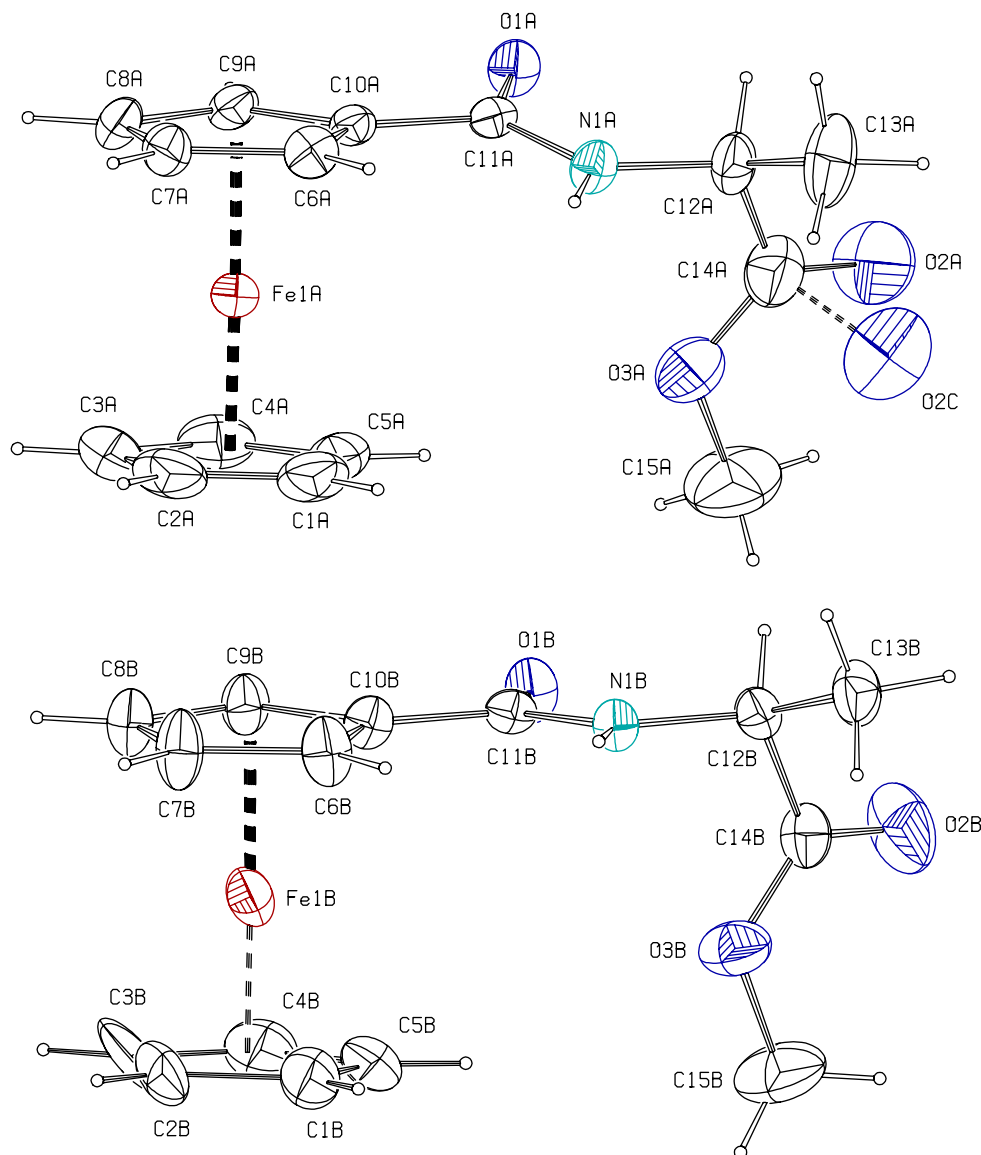


Fig. 3. An ORTEP diagram of the two independent molecules of **4** with the atomic displacement parameters depicted at the 50% probability level.

and related derivatives [7,12]. As can be evidenced by analysis of the interplanar angles which are  $16.7(2)^\circ$  and  $16.6(2)^\circ$  in the glycine methyl and benzyl ester derivatives, respectively, the overall molecular conformation is broadly similar in the ferrocenyl amide moieties.

### 3. Summary

The *N*-ferrocenoyl ester derivatives **1–10**, were prepared by coupling ferrocene carboxylic acid with the appropriate amino acid ester using the 1,3-dicyclohexylcarbodiimide (DCC), 1-hydroxybenzotriazole (HOBT) protocol and these have been characterised by spectroscopic techniques. It has been shown that the least sterically hindered ferrocenoyl glycine based ami-

no acid esters **1**, **2** and **3** give the optimum response both in the  $^1\text{H}$  NMR titration and the electrochemical studies in comparison to the bulkier *L*-Ala, *L*-Leu and *L*-Phe derivatives. The crystal structure of the *N*-ferrocenoyl-*L*-alanine methyl ester derivative **4** is also described.

### 4. Experimental

#### 4.1. General procedures

All chemicals were purchased from Sigma/Aldrich and used as received. Ferrocene carboxylic acid was prepared according to Reeves [29]. Amino acid ester hydrochlorides were prepared by the method of Brenner

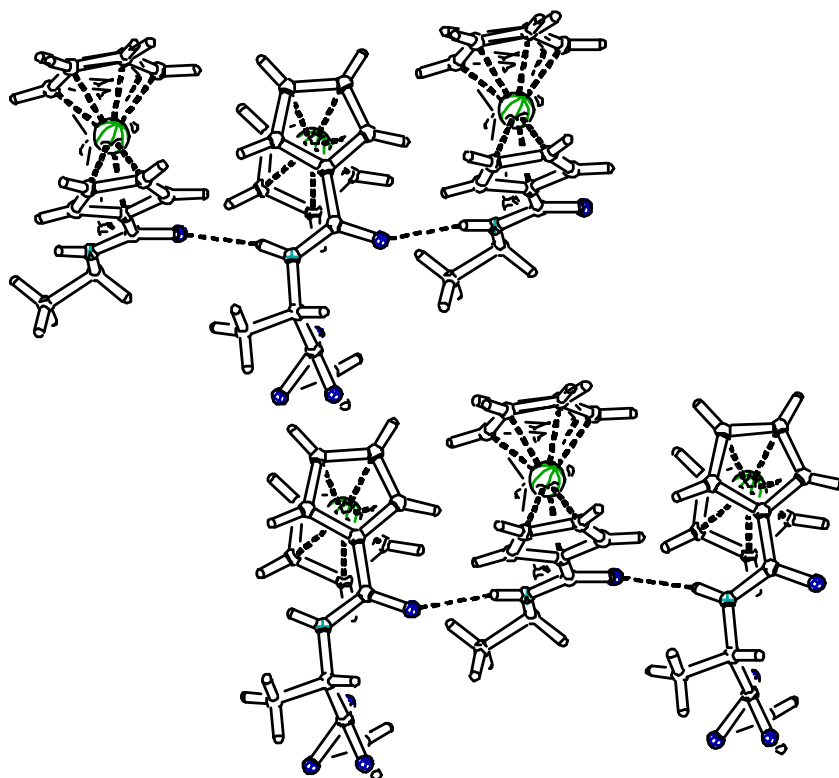


Fig. 4. A PLATON diagram depicting the intermolecular interactions in **4**.

and Huber [30]. Where necessary solvents were purified prior to use and stored under  $N_2$ , with  $CH_2Cl_2$  distilled from calcium hydride:  $Et_3N$  was distilled and stored over KOH pellets. Commercial grade reagents were used without further purification. Melting points were determined using a Griffin melting point apparatus and are uncorrected. Infrared spectra were recorded on a Nicolet 405 FT-IR spectrometer and UV-Vis spectra were recorded on a Hewlett-Packard 8452A diode array UV-Vis spectrophotometer. NMR spectra were obtained on a Bruker AC 400 FT-NMR spectrometer operating at 400 MHz for  $^1H$  and 100 MHz for  $^{13}C$  NMR. The  $^1H$  and  $^{13}C$  NMR chemical shifts (ppm) are reported downfield from tetramethylsilane (TMS) as internal standard and all coupling constants ( $J$ ) are in Hertz (Hz). Electrochemical studies were performed on a Bas 100/W electrochemical analyser equipped with a PA-100B/W low-current module for electrochemical measurements. The electrochemical cell was an unsealed one-compartment cell with a platinum microdisk (diameter 28  $\mu m$ ) working electrode, Ag/AgCl reference and platinum wire counter electrode and the experiments were conducted at 21  $^\circ C$ . Elemental analyses were performed in the Microanalytical Laboratory, University College Dublin. Positive ion fast atom bombardment mass spectra were obtained on the first of two sectors of a JEOL SX/SX 102 double focussing four sector tandem mass spectrometer with thioglycerol or

nitrobenzyl alcohol as the matrix: MALDI-TOF mass spectra were measured on a Kratos Kompact SEQ reflectron time of flight mass spectrometer using  $\alpha$ -cyano-4-hydroxycinnamic acid as the matrix.

#### 4.2. General procedure for the synthesis of *N*-ferrocenoyl amino acid esters: synthesis of *N*-ferrocenoyl glycine methyl ester (**1**)

Glycine methyl ester hydrochloride (1.08 g, 8.7 mmol) and triethylamine (1.22 ml, 8.7 mmol) ( $Et_3N$ ) were added to a solution of ferrocene carboxylic acid (2.00 g, 8.7 mmol), 1-hydroxy-benzotriazole (HOBt) (1.15 g, 8.7 mmol) and 1,3-dicyclohexylcarbodiimide (DCC) (1.80 g, 8.7 mmol) in dichloromethane (50 ml) at 0  $^\circ C$ . The reaction was allowed to reach room temperature after 30 min. and subsequently stirred for a further 48 h. The precipitated *N,N*-dicyclohexylurea was removed by filtration and the filtrate washed with water, 10%  $KHCO_3$ , 5% citric acid and dried over magnesium sulfate. The solvent was evaporated in vacuo and the resulting oil was recrystallised from ethyl acetate/pet. ether 40–60  $^\circ C$  to yield the title product as orange/brown rhomboids (1.16 g, 44%). The crystals were of sufficient quality for an X-ray diffraction study.

m.p. 127–128  $^\circ C$ .  $E_{1/2} = 603$  mV.

Mass spectrum: found:  $[M]^+$  301.02

$C_{14}H_{15}N_1O_3Fe$  requires: 301.04

IR  $\nu_{\max}$  KBr: 3257, 3086, 2937, 1753, 1639, 1541  $\text{cm}^{-1}$   
 UV-Vis,  $\lambda_{\max}$   $\text{CH}_3\text{CN}$ : 262, 304, 442 ( $\epsilon$  175) nm.

$^1\text{H}$  NMR (400 MHz)  $\delta$  (DMSO): 8.25 (1H, t,  $J = 6$  Hz,  $-\text{NH}-$ ), 4.78 (2H, t,  $J = 2$  Hz, *ortho*-H on substituted Cp ring), 4.35 (2H, t,  $J = 2$  Hz, *meta*-H on substituted Cp ring), 4.23 (5H, s, unsubstituted Cp ring), 3.90 (2H, d,  $J = 6$  Hz,  $-\text{NHCH}_2\text{CO}-$ ), 3.65 (3H, s,  $-\text{OCH}_3$ ).

$^{13}\text{C}$  NMR (100 MHz)  $\delta$  (DMSO): 170.6, 169.6, 75.5, 70.1, 69.4, 68.1, 51.6, 40.7.

#### 4.2.1. *N*-Ferrocenoyl glycine ethyl ester (2)

Glycine ethyl ester hydrochloride (1.20 g, 8.7 mmol) was used as starting material. Recrystallisation from ethyl acetate/pet. ether 40–60 °C yielded the title product as a yellow crystalline solid (1.53 g, 48%).

m.p. 140–141 °C.  $E_{1/2} = 601$  mV.

Analysis: found: C, 57.66; H, 5.62; N, 4.93.

$\text{C}_{15}\text{H}_{17}\text{N}_1\text{O}_3\text{Fe}$  requires: C, 57.17; H, 5.44; N, 4.45.

IR  $\nu_{\max}$  KBr: 3257, 3086, 1748, 1633, 1547  $\text{cm}^{-1}$

UV-Vis  $\lambda_{\max}$   $\text{CH}_3\text{CN}$ : 262, 304, 441 ( $\epsilon$  210) nm.

$^1\text{H}$  NMR (400 MHz)  $\delta$  (DMSO): 8.22 (1H, s,  $-\text{NH}-$ ), 4.71 (2H, t,  $J = 2$  Hz, *ortho*-H on substituted Cp ring), 4.36 (2H, t,  $J = 2$  Hz, *meta*-H on substituted Cp ring), 4.24–4.29 (7H, m, unsubstituted Cp ring and  $-\text{OCH}_2\text{CH}_3$ ), 4.15 (2H, d,  $J = 5$  Hz,  $-\text{NHCH}_2\text{CO}-$ ), 1.32 (3H, t,  $J = 7$  Hz,  $-\text{OCH}_2\text{CH}_3$ ).

$^{13}\text{C}$  NMR (100 MHz)  $\delta$  (DMSO): 170.6, 170.3, 75.1, 70.6, 69.8, 68.2, 61.5, 41.3, 14.2.

#### 4.2.2. *N*-Ferrocenoyl glycine benzyl ester (3)

Glycine benzyl ester tosylate (2.93 g, 8.7 mmol) was used. Recrystallisation from ethyl acetate/pet. ether 40–60 °C yielded a dark yellow crystalline solid (2.21 g, 68%). The crystals were suitable for an X-ray diffraction study.

m.p. 131–132 °C.  $E_{1/2} = 604$  mV.

Analysis: found: C, 63.49; H, 5.00; N, 3.64

$\text{C}^{20}\text{H}^{19}\text{N}^1\text{O}^3\text{Fe}$  requires: C, 63.68; H, 5.08; N, 3.71

Mass spectrum: found:  $[\text{M}]^+$  377.12

$\text{C}^{20}\text{H}^{19}\text{N}^1\text{O}^3\text{Fe}$  requires: 377.07

IR  $\nu_{\max}$  KBr: 3257, 3086, 1748, 1633, 1547  $\text{cm}^{-1}$ .

UV-Vis  $\lambda_{\max}$   $\text{CH}_3\text{CN}$ : 263, 303, 443 ( $\epsilon$  275) nm.

$^1\text{H}$  NMR (400 MHz)  $\delta$  ( $\text{CDCl}_3$ ): 7.32–7.37 (5H, m, ArH), 6.21 (1H, t,  $J = 5$  Hz,  $-\text{NH}-$ ), 5.21 (2H, s,  $-\text{OCH}_2\text{Ph}$ ), 4.69 (2H, t,  $J = 2$  Hz, *ortho*-H on substituted Cp ring), 4.34 (2H, t,  $J = 2$  Hz, *meta*-H on substituted Cp ring), 4.22 (5H, s, unsubstituted Cp ring), 4.18 (2H, d,  $J = 5$  Hz,  $-\text{NHCH}_2\text{CO}-$ ).

$^{13}\text{C}$  NMR (100 MHz)  $\delta$  ( $\text{CDCl}_3$ ): 170.7, 170.2, 135.1, 128.6, 128.5, 128.4, 75.0, 70.6, 69.8, 68.2, 67.2, 41.3.

#### 4.2.3. *N*-Ferrocenoyl-L-alanine methyl ester (4)

L-Alanine methyl ester hydrochloride (1.21 g, 8.7 mmol) was used. Recrystallisation from ethyl acetate yielded brown rhombic shaped crystals which were of sufficient quality for an X-ray diffraction study (1.99 g, 72%).

m.p. 161–162 °C.  $E_{1/2} = 599$  mV.  $[\alpha]_{\text{D}}^{25} = -22^\circ$  (10, EtOH).

Mass spectrum: found:  $[\text{M}]^+$  315.0773

$\text{C}_{15}\text{H}_{17}\text{N}_1\text{O}_3\text{Fe}$  requires: 315.0558

IR  $\nu_{\max}$  KBr: 3280, 3085, 2983, 1736, 1621, 1535  $\text{cm}^{-1}$ .

UV-Vis  $\lambda_{\max}$   $\text{CH}_3\text{CN}$ : 276, 302, 334, 442 ( $\epsilon$  132) nm.

$^1\text{H}$  NMR (400 MHz)  $\delta$  ( $\text{CDCl}_3$ ): 6.25 (1H, d,  $J = 7$  Hz,  $-\text{NH}-$ ), 4.69–4.75 (2H, m, *ortho*-H on substituted Cp and  $-\text{NHCHCO}-$ ), 4.64 (1H, dd,  $J_A = 3$  Hz,  $J_B = 2$  Hz, *ortho*-H on substituted Cp ring), 4.32–4.33 (2H, m, *meta*-H on substituted Cp ring), 4.20 (5H, s, unsubstituted Cp ring), 3.76 (3H, s,  $\text{OCH}_3$ ), 1.45 (3H, d,  $J = 7$  Hz,  $-\text{NHC(H)CH}_3\text{CO}-$ ).

$^{13}\text{C}$  NMR (100 MHz)  $\delta$  ( $\text{CDCl}_3$ ): 173.8, 169.9, 75.1, 70.6, 69.8, 68.4, 67.9, 52.4, 47.8, 18.6.

#### 4.2.4. *N*-Ferrocenoyl-L-alanine ethyl ester (5)

The synthetic procedure employed for **5** was identical to that for **4** except L-alanine ethyl ester hydrochloride (1.34 g, 8.7 mmol), was used. Recrystallisation from ethyl acetate yielded **5** as a bright yellow crystalline solid (1.85 g, 65%).

m.p. 129–130 °C.  $E_{1/2} = 598$  mV.  $[\alpha]_{\text{D}}^{25} = -28^\circ$  (15, EtOH).

IR  $\nu_{\max}$  KBr: 3269, 3086, 2983, 1742, 1621, 1535  $\text{cm}^{-1}$ .

UV-Vis  $\lambda_{\max}$   $\text{CH}_3\text{CN}$ : 274, 303, 442 ( $\epsilon$  176) nm.

$^1\text{H}$  NMR (400 MHz)  $\delta$  (DMSO): 8.04 (1H, d,  $J = 7$  Hz,  $-\text{NH}-$ ), 4.89 (1H, t,  $J = 1$  Hz, H *ortho* on Cp ring), 4.78 (1H, t,  $J = 1$  Hz, H *ortho* on Cp ring), 4.34–4.41 (3H, m, H *meta* on Cp ring and  $-\text{NHCHCO}-$ ), 4.21 (5H, s, unsubstituted Cp ring), 4.05–4.14 (2H, m,  $-\text{OCH}_2\text{CH}_3$ ), 1.35 (3H, d,  $J = 7$  Hz,  $-\text{NHC(H)CH}_3\text{CO}-$ ), 1.20 (3H, t,  $J = 7$  Hz,  $-\text{OCH}_2\text{CH}_3$ ).

$^{13}\text{C}$  NMR (100 MHz)  $\delta$  (DMSO): 172.9, 169.1, 75.6, 70.2, 70.1, 69.4, 68.6, 68.1, 60.4, 47.8, 16.9, 14.1.

#### 4.2.5. *N*-Ferrocenoyl-L-leucine methyl ester (6)

Compound **6** was prepared according to the method for **4** using L-leucine methyl ester hydrochloride (0.47 g, 2.6 mmol). Recrystallisation from ethyl acetate/pet. ether 40–60 °C furnished **6** as a yellow crystalline solid (1.01 g, 79%).

m.p. 136–137 °C.  $E_{1/2} = 603$  mV.  $[\alpha]_{\text{D}}^{25} = -47^\circ$  (20, EtOH).

IR  $\nu_{\max}$  KBr: 3326, 3086, 2960, 1748, 1627, 1530  $\text{cm}^{-1}$ .

UV–Vis  $\lambda_{\max}$  CH<sub>3</sub>CN: 270, 301, 442 ( $\epsilon$  121) nm.

<sup>1</sup>H NMR (400 MHz)  $\delta$  (CDCl<sub>3</sub>): 6.03 (1H, d,  $J$  = 8.4 Hz, –NH–), 4.74–4.80 (1H, m, –NHCHCO–), 4.71–4.72 (1H, m, H *ortho* on Cp ring), 4.64–4.65 (1H, m, H *ortho* on Cp ring), 4.33–4.34 (2H, m, H *meta* on Cp ring), 4.21 (5H, s, unsubstituted Cp ring), 3.75 (3H, s, –OCH<sub>3</sub>), 1.66–1.71 (2H, m, –CH<sub>2</sub>CH(CH<sub>3</sub>)<sub>2</sub>), 1.58–1.62 (1H, m, –CH<sub>2</sub>CH(CH<sub>3</sub>)<sub>2</sub>), 0.96 (6H, d,  $J$  = 6 Hz, –CH<sub>2</sub>CH(CH<sub>3</sub>)<sub>2</sub>).

<sup>13</sup>C NMR (100MHz)  $\delta$  (CDCl<sub>3</sub>): 174.3, 170.6, 75.6, 71.0, 70.1, 68.8, 68.4, 52.7, 50.8, 42.2, 25.4, 23.3, 22.3.

#### 4.2.6. *N-Ferrocenoyl-L-leucine ethyl ester (7)*

Compound **7** was prepared in a similar fashion to **4**, using L-leucine ethyl ester hydrochloride (1.70 g, 8.7 mmol). Recrystallisation from ethyl acetate furnished **7** as a light yellow crystalline solid (2.15 g, 66%).

m.p. 127–128 °C.  $E_{1/2}$  = 604 mV.  $[\alpha]_{\text{D}}^{25}$  = –27° (21, EtOH).

IR  $\nu_{\max}$  KBr: 3303, 3086, 2960, 1742, 1627, 1535 cm<sup>–1</sup>.

UV–Vis  $\lambda_{\max}$  CH<sub>3</sub>CN: 272, 302, 442 nm ( $\epsilon$  124).

<sup>1</sup>H NMR (400 MHz)  $\delta$  (CDCl<sub>3</sub>): 6.03 (1H, d,  $J$  = 8 Hz, –NH–), 4.74–4.79 (1H, m, –NHCHCO–), 4.71 (1H, s, H *ortho* on Cp ring), 4.64 (1H, s, H *ortho* on Cp ring), 4.34 (2H, s, H *meta* on Cp ring), 4.18–4.23 (7H, m, 5H, unsubstituted Cp ring and –OCH<sub>2</sub>CH<sub>3</sub>), 1.66–1.74 (2H, m, –CH<sub>2</sub>CH(CH<sub>3</sub>)<sub>2</sub>), 1.57–1.64 (1H, m, –CH<sub>2</sub>CH(CH<sub>3</sub>)<sub>2</sub>), 1.29 (3H, t,  $J$  = 7 Hz, –OCH<sub>2</sub>CH<sub>3</sub>), 0.97 (6H, d,  $J$  = 6 Hz, –CH<sub>2</sub>CH(CH<sub>3</sub>)<sub>2</sub>).

<sup>13</sup>C NMR (100 MHz)  $\delta$  (CDCl<sub>3</sub>): 173.5, 170.1, 75.3, 70.6, 70.5, 69.8, 68.4, 68.0, 61.4, 50.5, 42.0, 25.0, 22.9, 21.9, 14.2.

#### 4.2.7. *N-Ferrocenoyl-L-leucine benzyl ester (8)*

Compound **8** was prepared in a similar fashion to that described for **3** using L-leucine benzyl ester tosylate (0.79 g, 2.0 mmol). Recrystallisation from ethyl acetate/ether yielded **8** as an orange crystalline solid (0.53 g, 61%).

m.p. 112–113 °C.  $E_{1/2}$  = 607 mV.  $[\alpha]_{\text{D}}^{25}$  = –17° (22, EtOH).

Analysis: found: C, 66.69; H, 5.94; N, 3.73

C<sub>24</sub>H<sub>27</sub>N<sub>1</sub>O<sub>3</sub>Fe requires: C, 66.52; H, 6.28; N, 3.23

IR  $\nu_{\max}$  KBr: 3314, 2960, 1745, 1627, 1535 cm<sup>–1</sup>.

UV–Vis  $\lambda_{\max}$  CH<sub>3</sub>CN: 268, 304, 442 ( $\epsilon$  135) nm.

<sup>1</sup>H NMR (400 MHz)  $\delta$  (CDCl<sub>3</sub>): 7.31–7.38 (5H, m, ArH), 6.04 (1H, d,  $J$  = 8 Hz –NH–), 5.21 (2H, s, –OCH<sub>2</sub>C<sub>6</sub>H<sub>5</sub>), 4.82–4.87 (1H, m, –NHCHCO–), 4.72–4.73 (1H, m, H *ortho* on Cp ring), 4.65–4.66 (1H, m, H *ortho* on cp ring), 4.35–4.36 (2H, m, H *meta* on Cp ring), 4.21 (5H, s, unsubstituted Cp ring), 1.58–1.76 (3H, m, –CH<sub>2</sub>CH(CH<sub>3</sub>)<sub>2</sub>), 0.97 (6H, d,  $J$  = 6 Hz, –CH<sub>2</sub>CH(CH<sub>3</sub>)<sub>2</sub>).

<sup>13</sup>C NMR (100 MHz)  $\delta$  (CDCl<sub>3</sub>): 173.7, 170.7, 135.8, 129.0, 128.8, 128.7, 75.6, 71.0, 70.2, 68.8, 68.5, 67.5, 51.0, 42.1, 25.4, 23.4, 22.3.

#### 4.2.8. *N-Ferrocenoyl-L-phenylalanine methyl ester (9)*

Compound **9** was prepared in a similar fashion to **4** using L-phenylalanine methyl ester hydrochloride (1.77 g, 8.7 mmol). Recrystallisation from ethyl acetate gave **9** as a dark yellow solid (2.24 g, 68%).

m.p. 120–122 °C.  $E_{1/2}$  = 608 mV.  $[\alpha]_{\text{D}}^{25}$  = –12° (6, EtOH).

IR  $\nu_{\max}$  KBr: 3269, 3097, 1759, 1730, 1621, 1541 cm<sup>–1</sup>.

UV–Vis  $\lambda_{\max}$  CH<sub>3</sub>CN: 262, 300, 443 ( $\epsilon$ 191) nm.

<sup>1</sup>H NMR (400 MHz)  $\delta$  (CDCl<sub>3</sub>): 7.19–7.36 (5H, m, ArH), 6.05 (1H, d,  $J$  = 8 Hz, –NH–), 5.01–5.06 (1H, m, –NHCHCO–), 4.63 (1H, d,  $J$  = 1 Hz, H *ortho* on Cp ring), 4.59 (1H, d,  $J$  = 1 Hz, H *ortho* on Cp ring), 4.32 (2H, d,  $J$  = 1 Hz, H *meta* on Cp ring), 4.12 (5H, s, unsubstituted Cp ring), 3.78 (3H, s, –OCH<sub>3</sub>), 3.13–3.26 (2H, m, PhCH<sub>2</sub>CH–).

<sup>13</sup>C NMR (100 MHz)  $\delta$  (CDCl<sub>3</sub>): 172.3, 170.1, 136.0, 129.2, 128.7, 127.2, 75.3, 70.9, 70.5, 69.7, 68.3, 68.0, 52.8, 52.4, 38.0.

#### 4.2.9. *N-Ferrocenoyl-L-phenylalanine ethyl ester (10)*

**10** was prepared analogously to that described for **4** using L-phenylalanine ethyl ester hydrochloride (0.87 g, 4 mmol). Recrystallisation from ethyl acetate yielded the **10** as a yellow solid (1.04 g, 56%).

m.p. 149–151 °C.  $E_{1/2}$  = 607 mV.  $[\alpha]_{\text{D}}^{25}$  = –5° (2, EtOH).

Analysis: found: C, 65.34; H, 6.00; N, 3.31

C<sub>22</sub>H<sub>23</sub>N<sub>1</sub>O<sub>3</sub>Fe requires: C, 65.20; H, 5.72; N, 3.46

IR  $\nu_{\max}$  KBr: 3291, 3097, 1753, 1627, 1535 cm<sup>–1</sup>.

UV–Vis  $\lambda_{\max}$  CH<sub>3</sub>CN: 256, 302, 442 ( $\epsilon$  197) nm.

<sup>1</sup>H NMR (400 MHz)  $\delta$  (CDCl<sub>3</sub>): 7.20–7.35 (5H, m, ArH), 6.08 (1H, d,  $J$  = 7 Hz, –NH–), 4.99–5.04 (1H, m, –NHCHCO–), 4.63 (1H, s, H *ortho* on Cp ring), 4.59 (1H, s, H *ortho* on Cp ring), 4.33 (2H, s, H *meta* on cp ring), 4.22 (2H, q,  $J$  = 7 Hz, –OCH<sub>2</sub>CH<sub>3</sub>), 4.13 (5H, s, unsubstituted Cp ring), 3.14–3.25 (2H, m, PhCH<sub>2</sub>CH–), 1.29 (3H, t,  $J$  = 7 Hz, –OCH<sub>2</sub>CH<sub>3</sub>).

<sup>13</sup>C NMR (100MHz)  $\delta$  (CDCl<sub>3</sub>): 171.9, 170.0, 136.1, 129.3, 128.6, 127.2, 75.4, 70.8, 70.5, 69.7, 68.3, 68.0, 61.5, 52.8, 38.1, 14.2.

### 4.3. Electrochemical studies

Electrochemical measurements were performed in CH<sub>3</sub>CN with 0.1 M [<sup>n</sup>Bu<sub>4</sub>N][PF<sub>6</sub>] as supporting electrolyte. Cyclic voltammetry was performed in a three electrode cell using a platinum microdisk working elec-

trode, Ag/AgCl reference electrode and a platinum wire counter electrode. Compounds **1–10** exhibited a fully reversible one-electron oxidation attributed to ferrocene oxidation to the ferrocenium cation in the region +590 to +610 mV vs the Ag/AgCl electrode. Measurements were recorded after addition of stoichiometric equivalents of anion guests to the electrochemical solutions. Solutions were ca.  $1 \times 10^{-3}$  mol dm $^{-3}$  in concentration and potentials were determined at 21 °C, 50 mV s $^{-1}$  scan rate. Anodic shifts in the ferrocene–ferrocenium redox couple were produced by the presence of anion (10 equiv.) added as their [ $n$ Bu $_4$ N] $^+$  salts.

#### 4.4. Crystallographic footnote for (**4**)

*Crystallographic data:* Chemical formula C $_{15}$ H $_{17}$ FeNO $_3$ , molecular weight 315.15 g mol $^{-1}$ , monoclinic, space group P2 $_1$  (No. 4),  $a = 10.032(2)$ ,  $b = 10.143(2)$ ,  $c = 14.350(1)$  Å,  $\beta = 95.98(1)^\circ$ ,  $V = 1452.1(4)$  Å $^3$ ,  $Z = 4$ ,  $T = 296(1)$  K, density = 1.44 g cm $^{-3}$  (calc.),  $F(000) = 656$ ,  $\mu = 8.39$  cm $^{-1}$ ,  $\psi$ -scans absorption correction range 0.59–1.00, 2408 reflections to  $2\theta = 120^\circ$ , 2302 unique (with  $I > 2\sigma I$ ), 406 parameters,  $R$ -factor is 0.030,  $wR_2 = 0.078$  (based on  $F_2$  for with  $I > 2\sigma I$  using SHELXL97 as the refinement program [36],  $GOF = 1.04$ , density range in final  $\Delta$ -map is  $-0.25$  to  $+0.26$  e Å $^{-3}$ .

#### 5. Supplementary material

Crystallographic data (excluding structure factors) for **4** have been deposited with the Cambridge Crystallographic Data Centre as supplementary publication no. 192257. Copies of the data can be obtained free of charge, on application to the CCDC, 12 Union Road, Cambridge, CB2 1EZ, UK (fax: +44 (0) 1223-336033 or e-mail: [deposit@ccdc.cam.ac.uk](mailto:deposit@ccdc.cam.ac.uk)).

#### Acknowledgements

P.T.M.K. and M.J.S. thank Forbairt, Irish American Partnership and Dublin City University for the funding of a studentship award.

#### References

- [1] P.D. Beer, Acc. Chem. Res. 31 (1998) 71.  
 [2] V. Degani, A. Heller, J. Phys. Chem. 91 (1987) 1285.

- [3] A. Nomoto, T. Moriuchi, S. Yamazaki, A. Ogawa, T. Hirao, J. Chem. Soc., Chem. Commun. (1998) 1963.  
 [4] A. Chesney, M.R. Bryce, A.S. Batsanov, J.A.K. Howard, L.M. Goldenberg, J. Chem. Soc., Chem. Commun. (1998) 677.  
 [5] H. Plenio, C. Aberle, Organometallics 16 (1997) 5950.  
 [6] P.D. Beer, F. Szemes, V. Balzani, C.M. Sala, M.G.B. Drew, S.W. Dent, M. Maestri, J. Am. Chem. Soc. 119 (1997) 11864.  
 [7] H.-B. Kraatz, J. Lusztyk, G.D. Enright, Inorg. Chem. 36 (1997) 2400.  
 [8] H. Fink, N.J. Long, A.J. Martin, G. Opromolla, A.J.P. White, D.J. Williams, P. Zanello, Organometallics 16 (1997) 2646.  
 [9] T.J. Peckham, A.J. Lough, I. Manners, Organometallics 18 (1999) 1030.  
 [10] M. Kira, T. Matsubara, H. Shinohara, M. Sisido, Chem. Lett. (1997) 89.  
 [11] P. Saweczko, H.-B. Kraatz, Coord. Chem. Rev. 192 (1999) 185.  
 [12] H.-B. Kraatz, D.M. Leek, A. Houmam, G.D. Enright, J. Lusztyk, D.D.M. Wayner, J. Organomet. Chem. 589 (1999) 38.  
 [13] T. Moriuchi, A. Nomoto, K. Yoshida, T. Hirao, J. Organomet. Chem. 589 (1999) 50.  
 [14] J.F. Gallagher, P.T.M. Kenny, M.J. Sheehy, Inorg. Chem. Commun. 2 (1999) 200.  
 [15] J.F. Gallagher, P.T.M. Kenny, M.J. Sheehy, Inorg. Chem. Commun. 2 (1999) 327.  
 [16] O. Brosch, T. Weyhermuller, N. Metzler-Nolte, Eur. J. Inorg. Chem. 2 (2000) 323.  
 [17] A. Hess, J. Sehnert, T. Weyhermuller, N. Metzler-Nolte, Inorg. Chem. 39 (2000) 5437.  
 [18] T. Moriuchi, K. Yoshida, T. Hirao, Organometallics 20 (2001) 3101.  
 [19] Y.M. Xu, H.-B. Kraatz, Tetrahedron Lett. 42 (2001) 2601.  
 [20] T. Moriuchi, K. Yoshida, T. Hirao, J. Organomet. Chem. 637 (2001) 75.  
 [21] A. Wieckowska, R. Bilewicz, A. Misicka, M. Pietraszkiewicz, K. Bajdor, L. Piela, Chem. Phys. Lett. 350 (2001) 447.  
 [22] H.-B. Kraatz, Y.M. Xu, P. Saweczko, J. Organomet. Chem. 637 (2001) 335.  
 [23] T. Moriuchi, A. Nomoto, K. Yoshida, A. Ogawa, T. Hirao, J. Am. Chem. Soc. 123 (2001) 68.  
 [24] S. Maricic, U. Berg, T. Frejd, Tetrahedron 58 (2002) 3085.  
 [25] S. Maricic, T. Frejd, J. Org. Chem. 67 (2002) 7600.  
 [26] D. Savage, J.F. Gallagher, Y. Ida, P.T.M. Kenny, Inorg. Chem. Commun. 5 (2002) 1034.  
 [27] D.R. van Staveren, N. Metzler-Nolte, T. Weyhermuller, J. Chem. Soc., Dalton Trans. (2003) 210.  
 [28] J.F. Gallagher, P.T.M. Kenny, M.J. Sheehy, Acta Crystallogr. C 55 (1999) 1257.  
 [29] P.C. Reeves, Org. Synth. 56 (1977) 28.  
 [30] H. Brenner, W. Huber, Helv. Chim. Acta 36 (1953) 1109.  
 [31] P.D. Beer, A.D. Keefe, J. Organomet. Chem. C 40 (1989) 375.  
 [32] P.D. Beer, A.R. Graydon, A.O.M. Johnson, D.K. Smith, Inorg. Chem. 36 (1997) 2112.  
 [33] M.G. Boutelle, H. Allen, O. Hill, M. Berners, R. John, P.D. Dobson, P. Leigh, J. Mol. Recogn. 9 (1996) 664.  
 [34] D. Kriz, O. Ramstrom, A. Svensson, K. Mosbach, Anal. Chem. 67 (1995) 2142.  
 [35] K.P. Xiao, P. Buhlmann, S. Nishizawa, S. Amemiya, Y. Umezawa, Anal. Chem. 69 (1997) 1038.  
 [36] G.M. Sheldrick, SHELXL97, University of Göttingen, Göttingen, 1997.